

Curvature effect on seismic response of curved highway viaducts equipped with unseating cable restrainers

Carlos MENDEZ GALINDO ^{*}, Toshiro HAYASHIKAWA ^{**} and Daniel RUIZ JULIAN ^{***}

^{*} Graduate Student, Graduate School of Eng., Hokkaido University, Nishi 8 Kita 13 Kita-ku, Sapporo 060-8628

^{**} Dr. of Eng., Professor, Graduate School of Eng., Hokkaido University, Nishi 8 Kita 13 Kita-ku, Sapporo 060-8628

^{***} Postdoctoral Fellow, Graduate School of Eng., Hokkaido University, Nishi 8 Kita 13 Kita-ku, Sapporo 060-8628

This paper investigates the possibility of pounding, deck unseating and tangential joint residual damage depending on the curvature radius. Furthermore, an evaluation of the effectiveness of the use of cable restrainers on the overall 3D seismic response of highway viaducts is presented. For this purpose, the bridge seismic performance has been evaluated on four different radii of curvature, considering two cases: restrained and unrestrained curved viaducts. Depending on the radius of curvature, three-dimensional non-linear dynamic analysis shows the vulnerability of curved viaducts to pounding and deck unseating damage. In this study, the efficiency of using cable restrainers on curved viaducts is demonstrated, not only by reducing in all cases the possible damage, but also by providing a similar behavior in the viaducts despite of curvature radius.

Key Words: Nonlinear dynamic response, unseating prevention system, seismic design

1. Introduction

Recently, severe strong earthquakes have repeatedly demonstrated that during an earthquake, adjacent spans often vibrate out-of-phase, causing two different types of displacement problems. The first type is a localized damage caused by the spans pounding together at the joints. The second type occurs when the expansion joint separates, possibly allowing the deck superstructure to become unseated from the supporting substructure if the seismically induced displacements are excessively large. Furthermore, damaged expansion joints may substantially disrupt the post-earthquake serviceability of the bridge. Additionally, bridges with curved configurations may sustain severe damage owing to rotation of the superstructure or displacement toward the outside of the curve line during an earthquake¹⁾. For this reason, curved bridges have suffered severe damage in past earthquakes. The implementation of modern seismic protection technologies has permitted the seismic modernization of bridges through the installation of cable restrainers that provide connection between adjacent spans. The purpose is to prevent the unseating of decks from

top of the piers at expansion joints by limiting the relative movements of adjacent bridge superstructures. Moreover, cable restrainers provide a fail-safe function by supporting a fallen girder unseated in the event of a severe earthquake¹⁾.

In addition, another commonly adopted earthquake protection strategy consists of replacing the vulnerable steel bearing supports with seismic isolation devices. Among the great variety of seismic isolation systems, lead-rubber bearing (LRB) has found wide application in bridge structures. This is due to its simplicity and the combined isolation-energy dissipation function in a single compact unit. Even though the application of the mentioned earthquake protection techniques, the considerable complexity associated with the analysis of curved viaducts requires a realistic prediction of the structural response, especially under the extreme ground motions generated by earthquakes. Besides, the performance of this kind of structures under great earthquakes presents a variation in the behavior depending on the radius of curvature. The effect of the curvature plays also an important role in the seismic behavior of curved highway viaducts, by increasing the bridge vulnerabilities during an earthquake²⁾.

Therefore, the purpose of the present study is to analyze the overall performance of highway viaducts with different radii of curvature. The effect of curvature on deck unseating damage and pounding damage is analyzed. In addition, a comparison between restrained and unrestrained highway bridges is presented. The study combines the use of non-linear dynamic analysis with a three-dimensional bridge model to accurately evaluate the seismic demands on four radii of curvature in the event of severe earthquakes.

2. Analytical Model of Viaducts

The great complexity related to the seismic analysis of highway viaducts enhances a realistic prediction of the bridge structural responses. This fact provides a valuable environment for the non-linear behavior due to material and geometrical non-linearities of the relatively large deflection of the structure on the stresses and forces. Therefore, the seismic analysis of the viaduct employs non-linear computer model that simulates the highly non-linear response due to impacts at the expansion joints. Non-linearities are also considered for characterization of the non-linear structural elements of piers, bearings and cable restrainers.

The highway viaduct considered in the analysis is composed by a three-span continuous seismically isolated section connected to a single simply supported non-isolated span. The overall viaduct length of 160 m is divided in equal spans of 40 m, as represented in **Fig. 1-a**. The bridge alignment is horizontally curved in a circular arc. Four different radii of curvature are taken into consideration measured from the origin of the circular arc to the centerline of the bridge deck. Tangential configuration for both piers and bearing supports is adopted, respect to the global coordinate system for the bridge, shown in the figure, in which the X- and Y-axes lie in the horizontal plane while the Z-axis is vertical.

2.1. Deck Superstructure and Piers

The bridge superstructure consists of a concrete deck slab that rests on three I-shape steel girders, equally spaced at an interval of 2.1 m. The girders are interconnected by end-span diaphragms as well as intermediate diaphragms at uniform spacing of 5.0 m. Full composite action between the slab and the girders is assumed for the superstructure model, which is treated as a three-dimensional grillage beam system shown in **Fig. 2**.

The deck weight is supported on two different arrangements of five hollow box section steel piers. The first

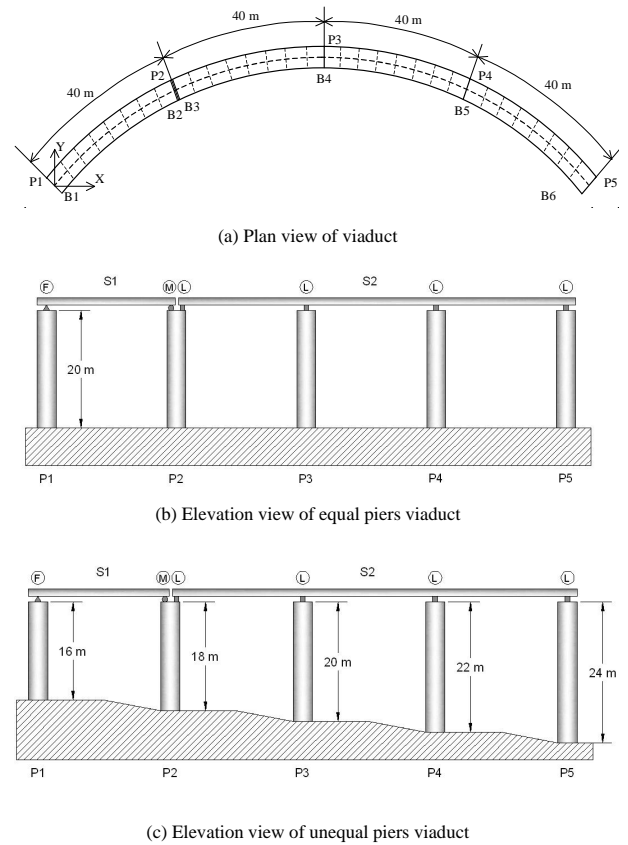


Fig. 1 Model of curved highway viaduct

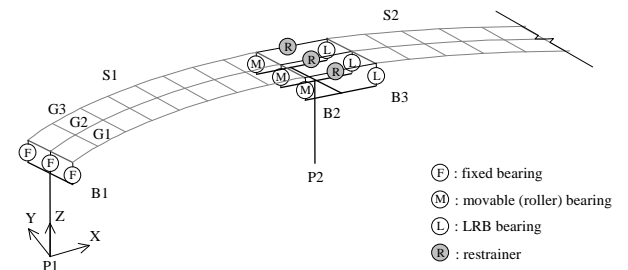


Fig. 2 Detail of curved viaduct finite element model

type, with equal piers of 20m height (EP), and the second with piers of 16m, 18m, 20m, 22m and 24m of height (UP), both cases designed according to the seismic code in Japan¹⁾, as is shown in **Figs. 1-b** and **1-c**. Cross sectional properties of the deck and the bridge piers are summarized in **Table 1**. Characterization of structural pier elements is based on the fiber element modelization where the inelasticity of the flexure element is accounted by the division of the cross-section into a discrete number of longitudinal and transversal fiber regions with constitutive model based on uniaxial stress-strain relationship for each zone. The element stress resultants are determined by integration of the fiber zone stresses over the cross section of the element. At the pier locations the viaduct deck is modeled in the transverse

direction as a rigid bar of length equal to the deck width. This transverse rigid bar is used to model the interactions between deck and pier motions³⁾.

2.2 Bearing Supports

Steel fixed bearing supports (**Fig. 3-a**) are installed across the full width on the left end of the simply-supported span (S1), resting on the Pier 1 (P1). Steel roller bearings at the right end on the Pier 2 (P2) allow for movement in the longitudinal (tangent to the curved superstructure) direction while restrained in the transverse radial direction. Coulomb friction force is taken into account in numerical analysis for roller bearings, which are modeled by using the bilinear rectangle displacement-load relationship, shown in **Fig. 3-b**.

The isolated continuous section (S2) is supported on four pier units (P2, P3, P4 and P5) by LRB bearings. The left end is resting on the same P2 that supports S1, and at the right end on top of P5. Orientation of LRB bearings is such as to allow for longitudinal and transverse movements. LRB bearing supports are represented by the bilinear force-displacement hysteresis loop presented in **Fig. 3-c**. The principal parameters that characterize the analytical model are the pre-yield stiffness K_1 , corresponding to combined stiffness of the rubber bearing and the lead core, the stiffness of the rubber K_2 and the yield force of the lead core F_1 . The structural properties of LRB supports are shown in **Table 2**. The devices are designed for optimum yield force level to superstructure weight ratio ($F_1/W = 0.1$) and pre-yield to post-yield stiffness ratio ($K_1/K_2 = 10.0$), which provide maximum seismic energy dissipation capacity as well as limited displacements⁴⁾.

It is also noted that properties of LRB bearings have been selected depending on the differences in dead load supported from the superstructure. The objective is to attract the appropriate proportion of non-seismic and seismic loads according to the resistance capacity of each substructure ensuring a near equal distribution of ductility demands over all piers. Furthermore, displacements of LRB bearings have been partially limited for all the viaducts, through the installation of lateral side stoppers.

2.3 Expansion Joint

The isolated and non-isolated sections of the viaduct are separated, introducing a gap equal to the width of the expansion joint opening between adjacent spans in order to allow for contraction and expansion of the road deck from creep, shrinkage, temperature fluctuations and traffic without generating constraint forces in the structure.

Table 1 Cross sectional properties of deck and piers

	$A \text{ (m}^2\text{)}$	$I_x \text{ (m}^4\text{)}$	$I_y \text{ (m}^4\text{)}^{(1)}$
P1	0.4500	0.3798	0.3798
P2	0.4700	0.4329	0.4329
P3	0.4700	0.4329	0.4329
P4	0.4700	0.4329	0.4329
P5	0.4500	0.3798	0.3798
G1	0.2100	0.1005	0.0994
G2	0.4200	0.1609	0.2182
G3	0.2100	0.1005	0.0994

⁽¹⁾ I_y in case of G1, G2 and G3

Table 2 Structural properties of LRB supports

Pier	K_1	K_2	F_1
Location	(MN/m)	(MN/m)	(MN)
P3, P4	49.00	4.90	0.490
P2, P5	36.75	3.68	0.368

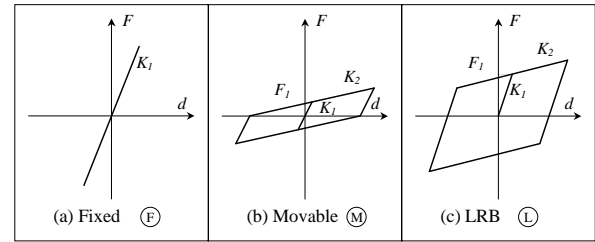


Fig. 3 Analytical models of bearing supports

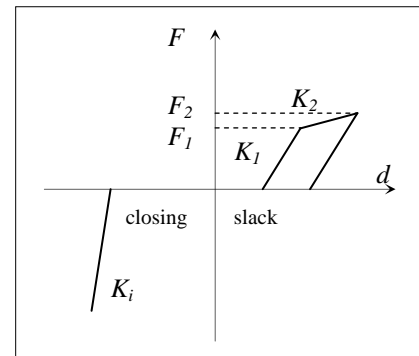


Fig. 4 Analytical model of the cable restrainer

In the event of strong earthquakes, the expansion joint gap of 0.1m could be closed resulting in collision between deck superstructures. The pounding phenomenon, defined as taking place at the three girder ends, is modeled using impact spring elements for which the compression-only bilinear gap element is provided with a spring of stiffness $K_i = 980.0 \text{ MN/m}$ that acts when the gap between the girders is completely closed.

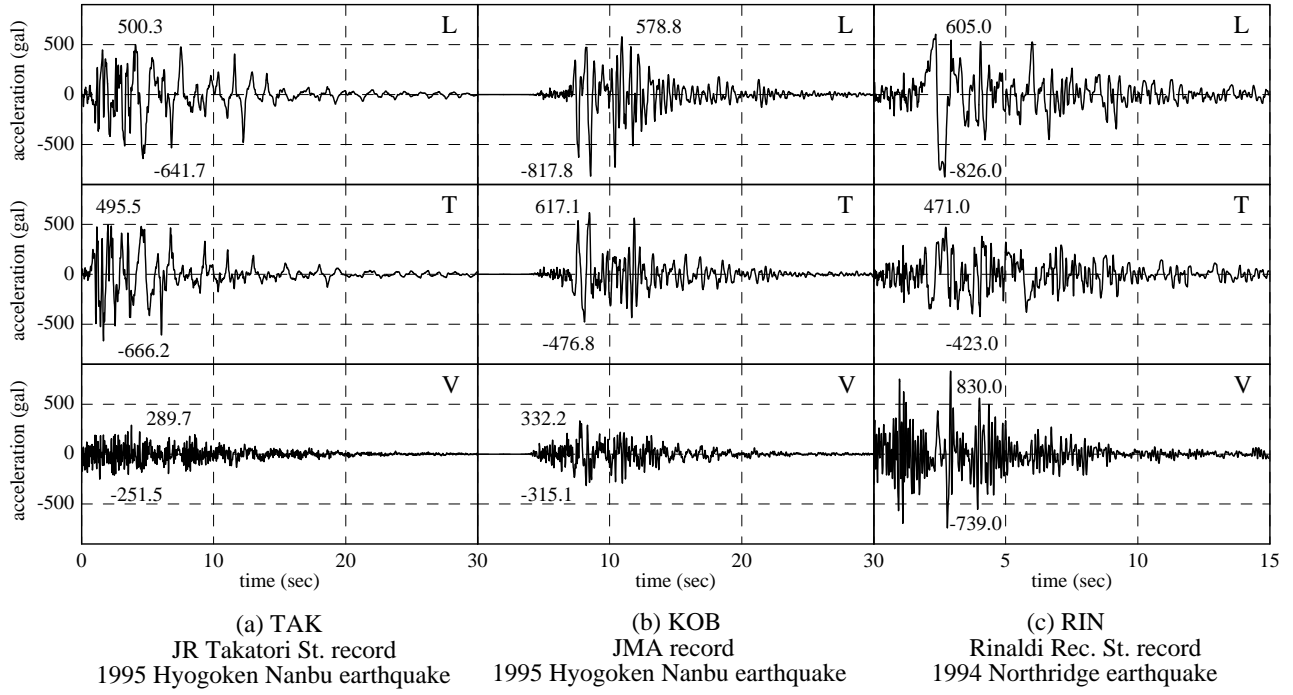


Fig. 5 Input earthquake ground motions

Table 3 Structural properties of cable restrainers

	Units	Value
E	(Gpa)	200
A	$\times 10^{-3} \text{ (m}^2\text{)}$	1.765
L	(m)	1.730
K_1	(MN/m)	204.058
K_2	(MN/m)	10.203
F_1	(MN)	2.584
F_2	(MN)	3.040

On the other hand, in the analysis of the restrained models, in order to prevent excessive opening of the expansion joint gap, it is provided additional fail-safe protection against extreme seismic loads; for this purpose, unseating cable restrainers units are anchored to the three girder ends (1 unit per girder) connecting both adjacent superstructures across the expansion joint. The seismic restrainers, illustrated in **Fig. 4**, have been modeled as tension-only spring elements provided with a slack of 0.025 m, a value fitted to accommodate the expected deck thermal movements limiting the activation of the system specifically for earthquake loading. Initially, restrainers behave elastically with stiffness K_1 , while their plasticity is introduced by the yield force (F_1) and the post-yielding stiffness ($K_2=0.05K_1$). Finally, the failure statement is taken into account for ultimate strength F_2 , and since then, adjacent spans can separate freely without any action of the

unseating prevention device. The structural properties of cable restrainer are presented in **Table 3**. In order to simplify, the effects of the expansion joint in the transverse direction as well as the shear forces acting on cable restrainers are neglected.

3. Method of Analysis

The bridge model is developed in-house using the Fortran programming language. The analysis on the highway bridge model is conducted using an analytical method based on the elasto-plastic finite displacement dynamic response analysis. The governing nonlinear equation of motion can be derived by the principle of energy that the external work is absorbed by the work of internal, inertial and damping forces for any small admissible motion that satisfies compatibility and essential boundary conditions⁵). Hence, the incremental finite element dynamic equilibrium equation at time $t+\Delta t$ over all the elements, can be expressed in the following matrix form:

$$[\mathbf{M}]\{\ddot{u}\}^{t+\Delta t} + [\mathbf{C}]\{\dot{u}\}^{t+\Delta t} + [\mathbf{K}]^{t+\Delta t}\{\Delta u\}^{t+\Delta t} = -[\mathbf{M}]\{\ddot{z}\}^{t+\Delta t} \quad (1)$$

where $[\mathbf{M}]$, $[\mathbf{C}]$ and $[\mathbf{K}]^{t+\Delta t}$ represent respectively the mass, damping and tangent stiffness matrices of the bridge structure at time $t + \Delta t$. While \ddot{u} , \dot{u} , Δu and \ddot{z} denote the

structural accelerations, velocities, incremental displacements and earthquake accelerations at time $t+\Delta t$, respectively. The incremental equation of motion accounts for both geometrical and material nonlinearities. Material nonlinearity is introduced through the bilinear elastic-plastic stress-strain relationship of the beam-column element, incorporating a uniaxial yield criterion and kinematic strain-hardening rule. The yield stress is 235.4 MPa, the elastic modulus is 200 GPa and the strain hardening in plastic area is 0.01.

Newmark's step-by-step method of constant acceleration is formulated for the integration of equation of motion. Newmark's integration parameters ($\beta=1/4$, $\gamma=1/2$) are selected to give the required integration stability and optimal result accuracy. The equation of motion is solved for the incremental displacement using the Newton-Raphson iteration scheme where the stiffness matrix is updated at each increment to consider geometrical and material nonlinearities and to speed to convergence rate. The damping mechanism is introduced in the analysis through the Rayleigh damping matrix, expressed as a linear combination of the mass matrix and the stiffness matrix. The particular values of damping coefficients are set to ensure a relative damping value of 2% in the first two natural modes of the structure.

To assess the seismic performance of the viaduct, the nonlinear bridge model is subjected to the longitudinal (L), transverse (T), and vertical (V) components of three strong ground motion records from the Takatori (TAK) and Kobe (KOB) Stations during the 1995 Kobe Earthquake, as well as Rinaldi (RIN) Station, from the Northridge Earthquake in 1994, as is given in **Fig. 5**. The longitudinal earthquake component shakes the highway viaduct parallel to the X-axis of the global coordinate system, while the transverse and vertical components are acting in the Y- and Z-axes, respectively. The large magnitude records from the 1995 Kobe Earthquake and Northridge Earthquake used in this study, classified as near-fault motions, are characterized by the presence of high peak accelerations and strong velocity pulses with a long period component as well as large ground displacements⁶⁾.

4. Numerical Results

The overall three-dimensional seismic responses of the viaducts are investigated in detail through non-linear dynamic response analysis. Particular emphasis has been focused on the expansion joint behavior due to the extreme

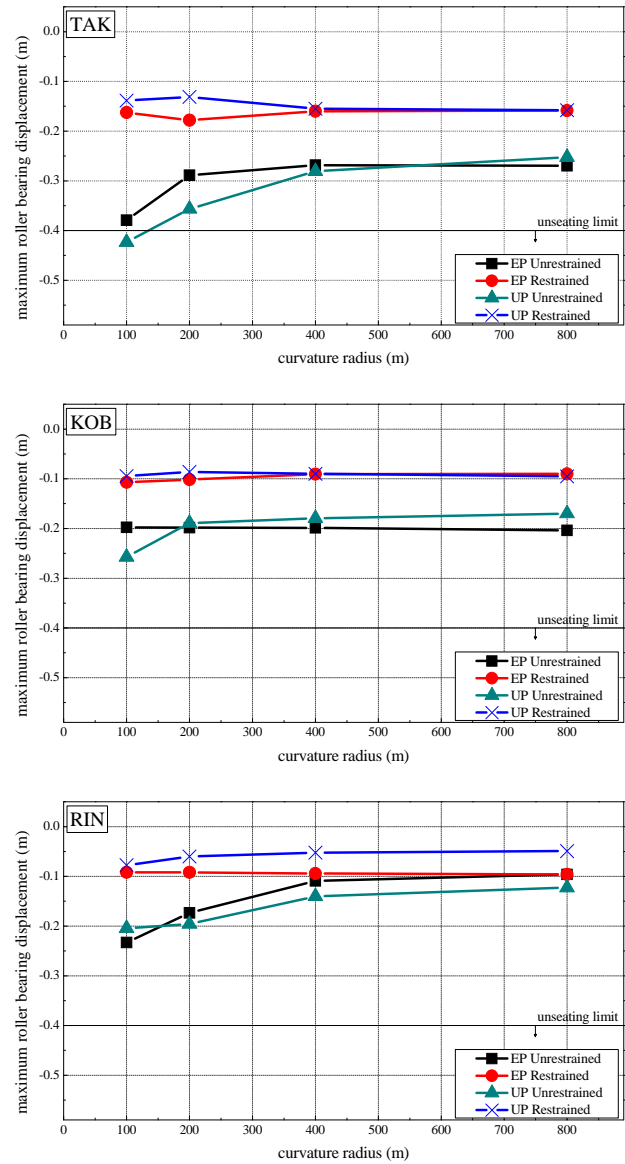


Fig. 6 Curvature effect on deck unseating damage

complexity associated with connection between isolated and non-isolated sections in curved viaducts. The bridge seismic performance has been evaluated on four different radii of curvature, 100 m, 200 m, 400 m, and 800 m, considering two cases: viaducts with and without unseating cable restrainers.

In the analysis of the restrained models, in order to prevent excessive opening of the expansion joint gap, unseating cable restrainers units are anchored to the three girder ends (one unit per girder) connecting both adjacent superstructures across the expansion joint. The seismic restrainers, illustrated in **Fig. 4**, have been modeled as tension-only spring elements provided with a slack of 0.025m, a value fitted to accommodate the expected deck thermal movements limiting the activation of the system specifically for earthquake loading.

4.1 Bearing Supports

Firstly, the effect of curvature radius on deck unseating damage is analyzed. During an earthquake, adjacent spans can vibrate out-of-phase, resulting in relative displacements at expansion joints. In simply-supported spans, the induced relative displacements to steel roller bearings can exceed the seat width at the pier top, causing the dislodgment of the rollers from the bearing assembly and the subsequent collapse due to deck superstructure unseating. The maximum roller bearing displacement in the negative tangential direction has been established as the damage index to evaluate the potential possibility of deck unseating. For this study, a limit of 0.40 m has been fixed to determine the high unseating probability for existing bridges with narrow steel pier caps that provide short seat widths.

First, the unrestrained viaducts are analyzed in terms of the maximum displacement on the steel roller bearing. The results, shown in **Fig. 6**, indicate that while none of the bridges in the equal piers overpass the unseating limit, dangerous displacements are observed, especially in the more curved viaducts. Moreover, a significant increment on the displacements is observed among the unequal piers viaducts, where the viaduct with 100m curvature radius overpasses the unseating limit for TAK input. It is easy to observe the increment on the displacements due to the use of piers with unequal heights, especially for TAK. Moreover, a close to limit maximum roller bearing displacement is observed in the bridge with radius of 200m, in contrast with the equal piers viaduct, in which the maximum displacement remains closer to the straight tending viaducts, 400m and 800m. In those viaducts, an acceptable displacement is observed in both cases, equal and unequal piers, and no high variation is presented in all inputs. It is clear that in case of more curved viaducts; the possibility of unseating damage is higher, especially in the more curved bridges. Therefore, it is possible to observe the significant reduction on the maximum displacements in the case of the bridges tending to the straight alignment.

For restrained viaducts, similar values of maximum displacements on the roller bearing are observed in both, equal and unequal piers viaducts. However, both cases present a remarkable reduction on the maximum displacements in comparison with the obtained in the unrestrained cases; particularly in the bridges with 100m curvature radius. From the results, it can be observed that the input record representing the worst scenario is TAK input, producing significantly higher displacements that put in risk the superstructure of the viaducts.

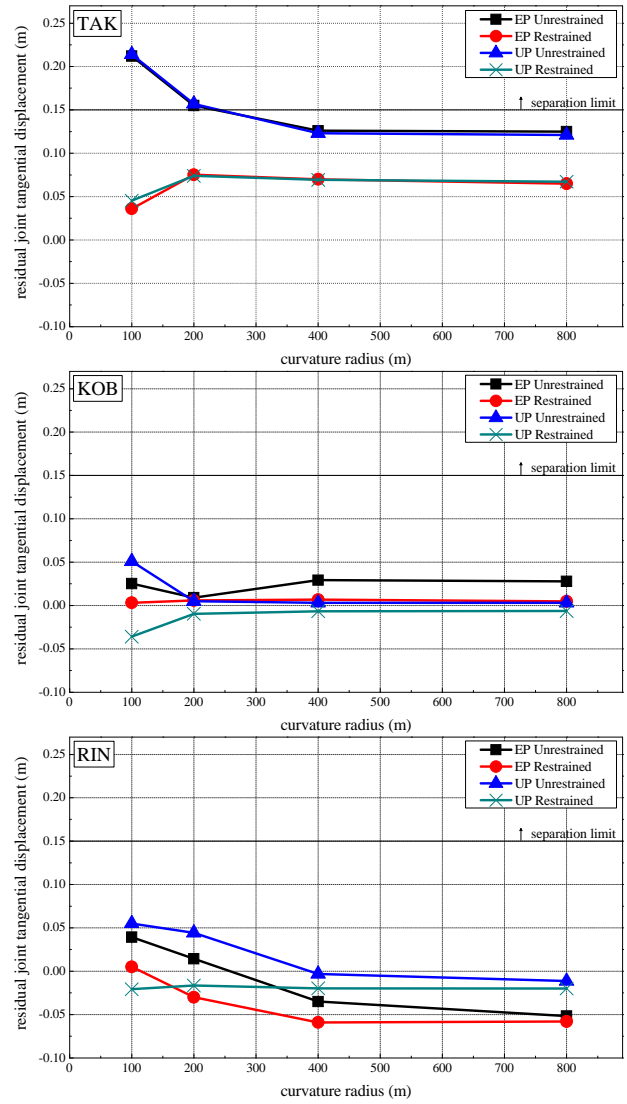


Fig. 7 Curvature effect on tangential joint residual damage

4.2 Expansion Joint Damage

Permanent tangential offsets at expansion joints cause, in several cases, traffic closure and the disruption of the bridge usability in the aftermath of the earthquakes resulted in a critical problem for rescue activities. This residual joint separation is mainly attributed to the final position of roller bearings supporting the superstructure. The relative inclination between adjacent piers, caused because seismic damages at the bottom of piers are not identical, has been also considered as an additional source of residual opening. The residual joint tangential displacement has been calculated in order to perform the post-earthquake serviceability evaluation on the viaduct. The possibility for vehicles to pass over the tangential gap length, measured as the contact length of a truck tire (0.15 m), is suggested as the limit for this damage. For unrestrained bridges, as shown in **Fig. 7**, the results of the residual joint tangential displacement show an important damage in the bridge with

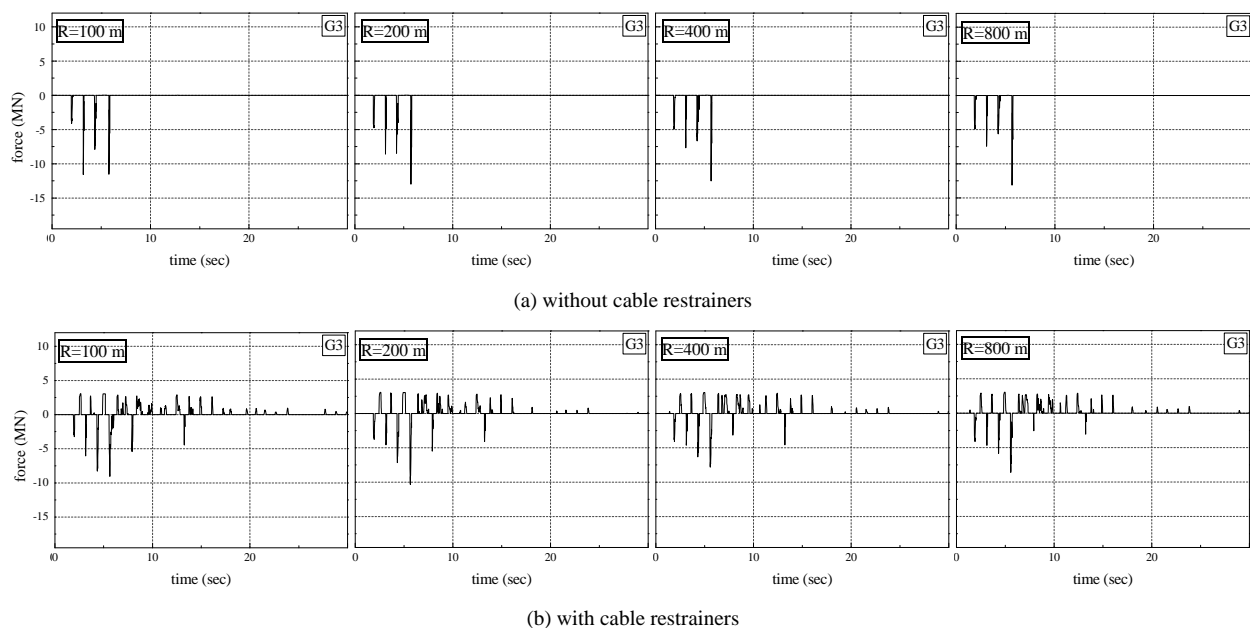


Fig. 8 Tangential residual damage from TAK in UP

100m and 200m curvature radii in both cases, equal and unequal piers viaducts. In TAK, the separation limit has been over passed, causing by this, the disruption on the bridge serviceability. KOB and RIN do not represent significant risk. Regarding the differences on the pier heights, there are no remarkable differences on the residual displacements. It is observed that as the curvature radius is increased, the behavior of the bridges tends to be less severe.

The results obtained from the analysis of the restrained viaducts are also shown in **Fig. 7**. The application of cable restrainers produces an important variation on the behavior of the bridges in comparison with the cases of unrestrained bridges. This effect is extensive for equal and unequal piers viaducts in all inputs. Firstly, a significant reduction in the tangential offsets of expansion joints is observed. For none of the bridges equipped with unseating prevention systems the separation limit of 0.15m is exceeded. In all the viaducts the residual displacement is observed under 0.08m. Clearly, the use of unseating prevention systems not only provides a residual displacement lower than the separation limit but also maintains these limits in similar values.

Another important problem presented in the expansion joint during the earthquake is the pounding damage. While seismic isolation provided by LRB bearings beneficially reduces the transmitted forces into the piers, the important added flexibility results in detrimental increase of collisions between adjacent decks. Due to this pounding phenomenon a remarkable point to note is that, in addition to the expected local damage at colliding girders, high impact forces are

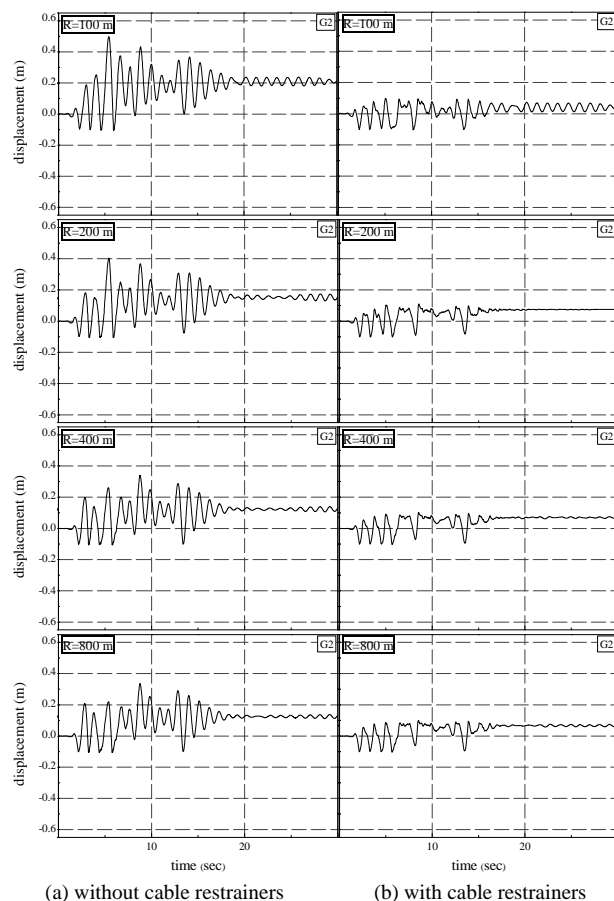


Fig. 9 Expansion joint relative displacement time-history from TAK in UP

transmitted to bearing supports located in the proximity of the expansion joint⁷⁾. The large spikes analytically observed in both, tangential and radial, components of reaction forces make the steel bearing supports particularly vulnerable to

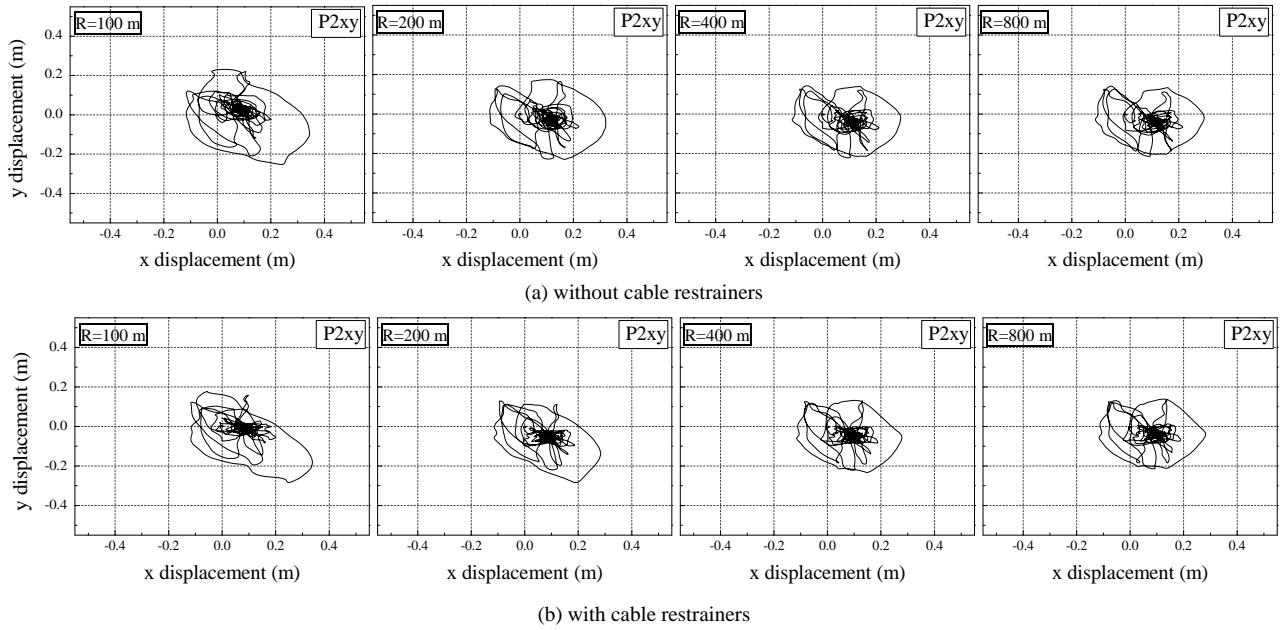


Fig. 10 Top displacements at P2 from TAK input in EP

failure, which could result into the collapse of the bridge. Ratios of maximum impact force to the deck weight greater than 1.0 have been observed to provide a good estimation of significant transmitted forces to bearing supports⁸⁾. Therefore, the effect of curvature radius on pounding damage is studied.

The analytical results for the unrestrained viaducts show that the higher number of impact forces are presented in the viaduct with unequal pier heights and curvature radius of 100m, followed by the bridge with 200m of curvature radius. The last two viaducts with 400m and 800m of curvature radii have impact forces significantly lower in most of the cases. It can be observed the uniform impact forces presented in the less curved viaducts with equal pier heights as well as in the case with unequal pier heights. **Fig. 8** shows the results from TAK, which represents the most severe condition. In case of the viaducts equipped with cable restrainers, the reduction in the possibility of pounding damage is significant. Firstly, the use of restrainers reduces the impact forces in all viaducts, despite the curvature radius and the differences on the pier heights; this can be noticed even in the bridge with radius of curvature of 100 m. This effect applies as well to the other bridges with 200m, 400m and 800m of curvature radii, as presented in **Fig. 8**. Therefore, it is possible to observe the remarkable advantages of the use of a deck unseating prevention system based on cable restrainers, especially in terms of pounding damage at the expansion joint. This significant improvement on the viaducts behavior can be observed as well in **Fig. 9**. The results indicate that the installation of cable restrainers

effectively reduces the relative displacements at the expansion joint, and therefore the possibility of pounding damage.

4.3 Pier at Expansion Joint

First, the effects of the curvature on the displacements at the top of the piers with equal heights are analyzed. For TAK input, which is the worst condition for the viaducts, the results show a significant effect of the curvature in term of displacements at the top of P2, it is clear how the more curved viaducts present a more severe condition in terms of movements at the pier top. In these cases, the bridge with curvature radius of 100 m is the most affected. A remarkable tendency to behave in a more suitable way can be noticed in straight tending bridges.

In **Fig. 10** it is also possible to observe the orientation of the displacements, which is in all the cases in the tangential direction. This is due to the installation of stoppers in order to limit the lateral displacements of the LRB bearings. On the other hand, in terms of the viaducts modeled with piers of unequal heights, the tendency of more curved bridges to suffer more severe displacements remains in all the viaducts. However, contrary to the results observed in the equal piers viaducts, in this case it is observed a higher impact of the use of cable restrainers. The pier top displacements presented on the restrained bridges are smaller than the ones obtained from the unrestrained viaducts. It is important to mention that for the viaducts with unequal piers, the results from inputs KOB and RIN remain considerable smaller than those observed in TAK.

5. Conclusions

The effects of curvature radius on nonlinear seismic response of curved highway viaducts equipped with cable restrainers have been analyzed. The possibility of seismic damage has been evaluated. Moreover, the effectiveness of cable restrainers to mitigate earthquake damage through connection between isolated and non-isolated sections of curved steel viaducts is evaluated. The investigation results provide sufficient evidence for the following conclusions:

The calculated results clearly demonstrate that curved viaducts are more vulnerable to deck unseating damage. However, this possibility is reduced by increasing the curvature radius or by the use of restrainers. Moreover, the use of cable restrainers provide to the bridge a similar behavior in case of curved and straight bridges, despite of the curvature radii and the differences on pier heights.

Curved viaducts are found vulnerable to tangential joint residual damage. The possibility increases by reducing the curvature radius. In restrained viaducts, a significant reduction of the residual joint tangential displacement is appreciated and similar values of residual joint tangential displacement are obtained. The use of piers with unequal heights does not denote higher displacements.

Also curved viaducts are found vulnerable to pounding damage. A significant reduction in the impact forces at the expansion joint is observed by increasing the curvature radius. Furthermore, even though the differences on the radii of curvature among the viaducts, the application of cable restrainers reduces the possibility of pounding damage. Finally, in this analysis, the effectiveness on the use of cable restrainers on curved viaducts is demonstrated, not only by reducing in all cases the possible damage but also by providing a similar behavior in the viaducts despite of curvature radius.

References

- 1) Japan Road Association (JRA), *Specifications for Highway Bridges – Part V Seismic Design*, Maruzen, Tokyo, 2002.
- 2) Robinson, W. H., Lead-rubber hysteretic bearings suitable for protecting structures during earthquakes, *Earthquake Engineering Structures*, Vol. 10, pp. 593-604, 1982.
- 3) Maleki, S., Effect of deck and support stiffness on seismic response of slab-girder bridges, *Engineering Structures*, Vol. 24, No. 2, pp. 219-226, 2002.
- 4) Mendez Galindo C., Hayashikawa T., Ruiz Julian F.D., Effects of curvature radius on nonlinear seismic response of curved highway viaducts equipped with unseating prevention cable restrainers, *Journal of Constructional Steel*, JSSC, Vol. 14, pp. 91-98, 2006.
- 5) Ali HM, Abdel-Ghaffar AM. Modeling the nonlinear seismic behavior of cable-stayed bridges with passive control bearings. *Computer & Structures*, Vol. 54, No.3, pp. 461-92, 1995.
- 6) Somerville P.G., Magnitude scaling of the near fault rupture directivity pulse. *Physics of the Earth and Planetary Interiors*, Vol. 137, pp. 201-12, 2003.
- 7) Zhu P., Abe M., Fujino Y., Evaluation of pounding countermeasures and serviceability of elevated bridges during seismic excitation using 3D modeling. *Earthquake Engineering & Structural Dynamics*, Vol.33, No.5, pp.591-609, 2004.
- 8) Mendez Galindo C., Hayashikawa T., Ruiz Julian F.D., Pounding and deck unseating damage of curved highway viaducts with piers of unequal heights, *Journal of Constructional Steel*, JSSC, Vol. 15, pp. 285-292, 2007.

(Received September 18, 2007)